JAAS

RSC Publishing

PAPER

View Article Online
View Journal | View Issue

Cite this: *J. Anal. At. Spectrom.*, 2013, **28**, 573

Rare earth element analysis in natural waters by multiple isotope dilution – sector field ICP-MS†

Tristan C. C. Rousseau,*[a] Jeroen E. Sonke,[a] Jerome Chmeleff,[a] Frederic Candaudap,[a] François Lacan,[b] Geraldo Boaventura,[c] Patrick Seyler[a] and Catherine Jeandel[b]

Received 1st November 2012
Accepted 4th February 2013

DOI: 10.1039/c3ja30332b

www.rsc.org/jaas

The rare earth elements (REEs) are valuable tracers in the earth, ocean and environmental sciences. Ten out of fourteen stable REEs have two or more isotopes, making them suitable for quantification by isotope dilution. We present a plasma mass spectrometry based multiple isotope dilution method for high precision REE concentration analysis in aqueous media. Key aspects of the method are: (i) flexible spiking of ten REEs *via* two LREE and HREE mixed spike solutions. (ii) Offline pre-concentration and matrix removal, by ion chromatography for freshwater samples and by iron co-precipitation or ion chromatography with the Nobias™ resin for seawater samples. (iii) High sensitivity detection by sector field-inductively coupled plasma mass spectrometry (SF-ICP-MS). (vi) The use of a desolvation micro-nebulization introduction system to lower polyatomic Ba and LREE-oxide interferences on HREEs. The method is suitable for a range of freshwater to seawater type samples, and was validated against SLRS-4, SLRS-5, and CASS-5 reference materials and two GEOTRACES marine inter-comparison samples. Long-term external precision on all REEs was <2% RSD, except La and Ce. Minimum sample volumes are 1 ml for freshwater and 50 ml for seawater. The multispike SF-ICP-MS method should be of particular interest in exploring subtle variations in aqueous REE fractionation patterns and anomalies in large numbers of samples.

1 Introduction

Rare Earth Elements (REEs) in rocks and sediments are tracers of crustal differentiation or palaeoproxies for seawater REE composition.[1–4] In natural waters REEs – together with Nd isotopes – are tracers of lithogenic inputs, solute–particle interactions, redox processes, and water mass mixing and circulation.[5–11]

To first order, the aqueous geochemistry of the REE is governed by the lanthanide contraction effect, *i.e.* the gradual decrease in ionic radii from La to Lu. Yet, both in experimental and natural systems complex REE trends are observed that require different explanations. Examples are middle REE (MREE) enrichment in Amazon River waters that have been linked to preferential dissolution of MREE-enriched phosphate minerals,[12] or the so-called tetrad effect in seawater samples.[13] In addition to redox related Ce anomalies in most natural waters, observations of natural Gd and Tb anomalies in seawater[14] and evidence of anthropogenic La and Gd anomalies have been reported.[15,16] Both the tetrad effect and the seawater Gd and Tb anomalies have been questioned due to analytical limitations and normalization issues.[17] Detecting subtle changes in REE patterns and REE anomalies in these fractions often requires final uncertainties better than 2% RSD.

There are several methods for REE concentration determination in natural waters. Initially highly precise, yet time consuming analyses were made by isotope dilution (ID) thermal ionization mass spectrometry.[8,18] While ID avoids quantification problems due to losses of REE during sample preparation, this method required laborious matrix and intra-REE separations due to a limited Faraday cup configuration flexibility and the need to avoid interferences.[19–21] One could typically determine three REEs at the same time, and mono-isotopic REEs were not measured by this method.

In the 1990s, the advent of inductively coupled plasma mass spectrometers (ICP-MS) provided much faster yet less precise analyses. REE concentration determination by quadrupole (Q-) ICP-MS using external calibration yields typical RSD's of 5–15%. Despite relatively low detection limits, oxide interferences in REEs, and matrix effects, Q-ICP-MS has been the key in exploring REE cycling in continental waters.[22–25] The use of sample aerosol desolvating devices as ICP-MS introduction systems has been shown to enhance sensitivity and limit Ba and light REEs (LREEs) oxide interferences on heavy REEs (HREEs).[26] Finally, single and

[a]*GET, Université de Toulouse, CNRS, IRD, CNES, 14 Avenue Edouard Belin, F-31400 Toulouse, France. E-mail: tristanrousseau@yahoo.fr*

[b]*LEGOS, Université de Toulouse, CNRS, IRD, CNES, 14 Avenue Edouard Belin, F-31400 Toulouse, France*

[c]*Universidade De Brasilia, UNB, LAGEQ, Campus universitario Darcy Ribeiro, 70.910-900 Brasilia, DF, Brazil*

† Electronic supplementary information (ESI) available: The ESI contains details on the spike calibration with MC-ICP-MS and further details on the multispike method (spiking strategy, setup, performances and data treatment). See DOI: 10.1039/c3ja30332b

multi-collector sector field mass spectrometers (SF-ICP-MS) have higher sensitivity than Q-ICP-MS, making them more suitable for ultra-trace REE analysis. Following dilution of seawater in order to lower the matrix ion concentrations introduced in the plasma, and using a desolvator to limit oxide interferences, it has been possible to directly measure REEs in coastal seawater.[27] However, REE determination in open ocean waters at the parts-per-quadrillion (ppq) level requires additional pre-concentration and matrix separation methods. A classic protocol is $Fe(OH)_3$ co-precipitation followed by an anionic chromatography column to remove Fe.[28,29] Solvent extraction or solid phase extraction using complexation resins is also a means of REE pre-concentration and separation.[30,31] Recently a new ion-exchange protocol was developed for direct REE pre-concentration from seawater using the new Nobias resin.[32–34]

Sensitivity variations and matrix effects can be monitored and corrected for by adding internal standards (In, Re, Tm).[35,36] The challenge of REE pre-concentration methods for ICP-MS analysis is to avoid or account for REE losses during the chemical processing. Isotope dilution using 2 or more REEs to correct such losses produces satisfactory results.[11,37] Nevertheless, a recent seawater intercomparison study of the REEs showed that inter-laboratory REE concentrations do not reproduce better than 10% 2RSD.[38] In 2002, the first multispike method suitable for SF-ICP-MS was published for rock analyses with a multi-collector ICP-MS (MC-ICP-MS).[39] The method is based on the addition of 10 enriched REE spikes to a rock digest, followed by a cationic column separation of LREE and HREE fractions to avoid oxide interferences of LREEs in HREEs. Baker *et al.*[39] (2002) achieved long-term external reproducibilities on all REEs that were <1% 2RSD. A method including 6 enriched REE spikes on a single collector SF-ICP-MS operated in high resolution mode on oxide interfered isotopes was published for rock analyses with a precision <5% 2RSD.[40,41]

We present here a precise and accurate method for REE analysis in natural waters by isotope dilution using 10 enriched REE spikes with a single collector SF-ICP-MS coupled with a desolvating introduction system. The method is inspired by the Baker *et al.* (2002) study, but uses a desolvation introduction system with additional N_2 gas to limit oxide interferences, and different REE pre-concentration protocols. Our method is suitable for a range of natural water types, *i.e.* river, ground, or seawater with final uncertainties better than 2% RSD for most REEs.

In the following we discuss isotope dilution principles, spiking strategy, separation/pre-concentration methods and instrument setup. Then, interference corrections and concentration calculations including mono-isotopic REEs (Pr, Tb, Ho, Tm) are detailed. Finally we present and discuss results of this method applied to reference river water, coastal seawater and open ocean seawater.

2 Materials and methods

2.1 Multispike REE method

Sample preparation and sample analysis procedures of the multispike method presented hereafter are summarized in Fig. 1. This method was validated by analyzing reference solutions provided by the Canadian National Research Council (CNRC): SLRS-4 and SLRS-5 riverine water, CASS-5 coastal water and two seawater samples collected in the framework of the GEOTRACES intercalibration program: one from the surface, the other at 2000 m depth, both collected at 31°50'N, 64°10'W (BATS station: Bermuda Atlantic Time-series Study, http://ijgofs.whoi.edu/Time-Series/BATS_presentation.pdf).

The REE analysis method we present here consists of simultaneous addition of known amounts of ten enriched REE isotope spikes to a sample (La, Ce, Nd, Sm, Eu, Gd, Dy, Er, Yb, and Lu). In the remainder we refer to the method as the REE 'multispike method'. Subsequently, we measure the ratios of ten pairs of REE isotopes in the sample/spike mixture by SF-ICP-MS. The concentrations of the ten corresponding REEs of natural isotopic composition in the sample are determined by the classical ID equation:

$$[\mathrm{REE}]_{\mathrm{smp}} = [\mathrm{REE}]_{\mathrm{spike}} \frac{W_{\mathrm{spk}}}{W_{\mathrm{smp}}} \frac{M_{\mathrm{nat}}}{M_{\mathrm{spk}}} \frac{A2_{\mathrm{spk}}}{A2_{\mathrm{nat}}} \frac{\left(\frac{A1_{\mathrm{spk}}}{A2_{\mathrm{spk}}} - R_{\mathrm{mix}}\right)}{\left(R_{\mathrm{mix}} - \frac{A1_{\mathrm{nat}}}{A2_{\mathrm{nat}}}\right)} \quad (1)$$

W_{smp}: mass in g of the sample.

W_{spk}: mass in g of the spike added to the sample.

M_{smp}: "Natural" NIST REE atomic mass.

M_{spk}: spike atomic mass.

$A1_{\mathrm{nat}}, A2_{\mathrm{nat}}, A1_{\mathrm{spk}}, A2_{\mathrm{spk}}$: natural spike relative abundances of isotopes 1 and 2.

R_{mix}: mass bias corrected ratio of isotope$_1$/isotope$_2$ in the sample/spike mix measured by SF-ICP-MS.

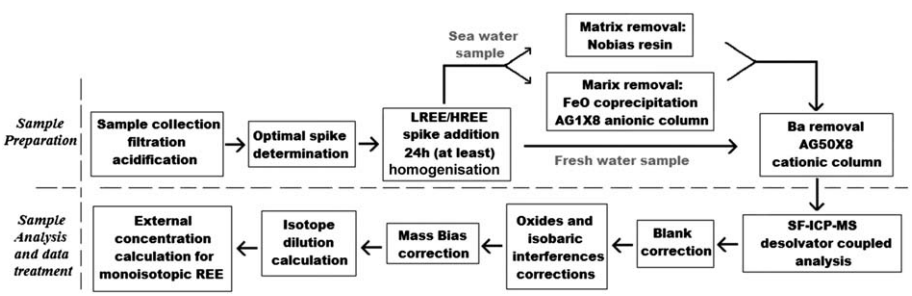

Fig. 1 Methodological scheme of multispike REE analysis of natural water samples on a single collector sector field ICP-MS.

The multispike calibration for isotopic composition (IC) and concentrations was done with a Thermo-Finnigan Neptune MC-ICP-MS. Details of the calibration are reported in the ESI.† Isotope pairs and associated natural and spike isotope abundances chosen for isotope dilution, along with atomic masses are reported in Table 1. The ideal amount of enriched spike to be added to a sample can be determined by evaluating the uncertainty magnification factor, M:

$$M = \frac{\left(\frac{A1_{nat}}{A2_{nat}} - \frac{A1_{spk}}{A2_{spk}}\right)R_{mix}}{\left(R_{mix} - \frac{A1_{nat}}{A2_{nat}}\right)\left(\frac{A1_{spk}}{A2_{spk}} - R_{mix}\right)} \quad (2)$$

This uncertainty level can be minimized as follows:

$$\frac{dM}{dR_{mix}} = 0 \quad (3)$$

We obtain the ideal R_{mix}:

$$R_{mix\text{-}idea} = \sqrt{\frac{A1_{spk}}{A2_{spk}}\frac{A1_{nat}}{A2_{nat}}} \quad (4)$$

A discussion of the uncertainty magnification factor and ideal $R_{mix\text{-}ideal}$ is reported in the ESI.†

Finding the optimum spike concentration requires a good idea of the approximate REE concentrations in an unknown sample. However, as discussed below, a certain amount of overspiking or underspiking can be tolerated without much increase of the final uncertainty on REE concentrations. Natural water samples display a variety of REE concentrations and spectra. We therefore chose to add the enriched REE spikes to the samples by using two mixed spike solutions. One containing the light to middle rare earth element spikes La, Ce, Nd, Sm, Eu, Gd, hereafter called 'mixed LREE spikes' and one containing Dy, Er, Yb, Lu, hereafter called 'mixed HREE spikes'. The relative spike concentrations in the mixed LREE and HREE spikes were chosen to display optimal R_{mix} when mixed with a simulated reference solution. This simulated reference solution when normalized to Post-Archean Average Australian Shale (PAAS)[42] displays REE spectra that we call 'central spectra'. The determination of the central spectra was made using the central relative value between extreme values of each REE within a compilation of distinct REE patterns of natural waters (seawater, Amazon river tributaries) normalized by the same Nd value for the LREEs and Er for the HREEs (Fig. 2a and b). Subsequently, the optimal LREE and HREE spike mixes were numerically tested to assure adequate spiking of all REE. In this step, the sensitivity of ID uncertainty was tested on the "central spectra" and on "natural spectra" to several levels of overspiking and underspiking (Fig. 3).

Staying within the 2% uncertainty magnification on final REE concentrations using the ID method allows overspiking of 3 times for Yb to 11 times for Sm and underspiking of 4 times for Eu to 15 times for Dy. The 4% to 2% uncertainty magnification difference being higher for overspiking than underspiking, overspiking would always be preferred to underspiking.

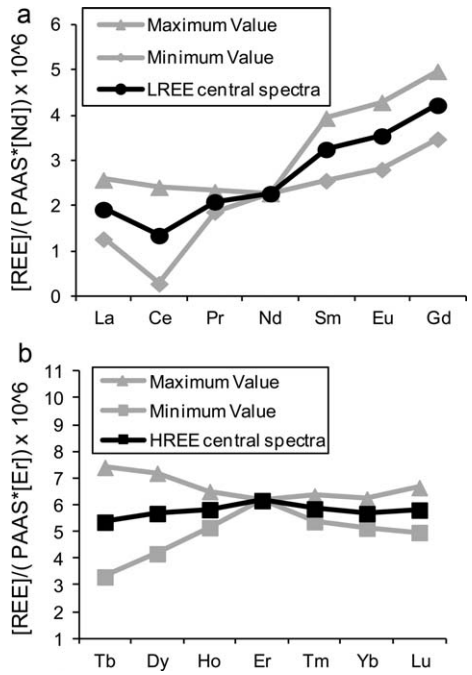

Fig. 2 Central PAAS normalized REE spectra with a compilation of river water and seawater REE patterns: (a) Nd normalized LREEs and (b) Er normalized HREEs.

Table 1 REE isotope abundances, ratios and atomic weights of natural and enriched isotope standard solutions. Ab = abundance, M_n = atomic mass of the natural REE element, M_s = atomic mass of the spike REE. 'nat' and 'spk' refer to natural and spike respectively

	$Isotope_1$	$Isotope_2$	$Ab.1_{nat}$	$Ab.2_{nat}$	$Ab.1_{spk}$	$Ab.2_{spk}$	M_n	M_s	$\frac{Ab1_{nat}}{Ab2_{nat}}$	$\frac{Ab1_{spk}}{Ab2_{spk}}$
La	138	139	0.09%	99.91%	6.76%	93.24%	138.91	138.84	0.0009	0.0725
Ce	136	140	0.19%	88.45%	24.342%	69.85%	140.12	139.01	0.0021	0.3485
Nd	146	145	17.18%	8.29%	97.35%	0.52%	144.24	145.88	2.0721	186.4034
Sm	149	147	13.82%	14.99%	96.72%	0.22%	150.37	148.94	0.9219	429.9969
Eu	151	153	47.81%	52.19%	97.70%	2.30%	151.96	150.97	0.9161	42.5030
Gd	157	155	15.65%	14.80%	91.66%	0.24%	157.25	156.97	1.0574	375.7594
Dy	163	161	24.90%	18.89%	95.60%	0.14%	162.50	162.90	1.3180	678.3316
Er	167	166	22.95%	33.60%	95.37%	1.27%	167.26	166.96	0.6830	75.0720
Yb	172	171	21.83%	14.28%	95.84%	1.31%	173.04	171.97	1.5287	73.3741
Lu	176	175	2.59%	97.41%	74.49%	25.51%	174.97	175.69	0.0266	2.9196

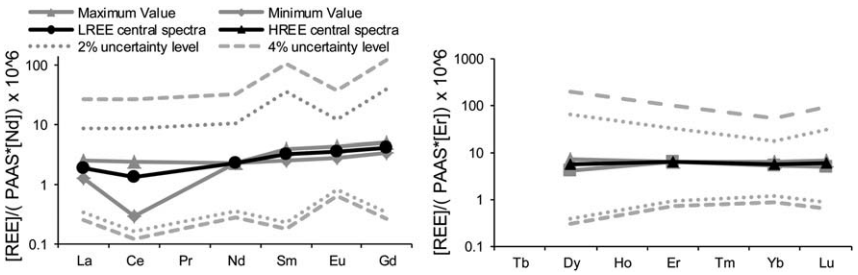

Fig. 3 2% and 4% uncertainty levels due to overspiking and underspiking of the "central spectra" reference REE patterns with the LREE and HREE mixed spike solutions.

The relative spike concentrations in mixed HREE and LREE spikes were also adjusted to minimize the isobaric and oxide interferences induced by the spike addition. We also aimed to obtain the same order of magnitude of signal within each pair of isotopes to assure that they were measured in the same SF-ICP-MS counting mode, *i.e.* pulse or analogue mode.

Consequently, some REE spikes were slightly and voluntary under or overspiked. For La and Lu, overspiking allowed us to minimize the isobaric interferences of Ba and Yb respectively. Nd, Sm and Dy were slightly underspiked to lower the quantity of Nd and Sm oxide interferences on HREEs and to reduce the difference of the signal between Dy isotopes. For routine analyses, the amounts of LREE and HREE spike mixes added to the sample are calculated by determining the optimal Nd and Er spiking. This requires a prior knowledge of the approximate Nd and Er concentrations in the sample within a 300% confidence interval.

2.2 Preconcentration, matrix removal, and Ba separation

REE analyses by ICP-MS of freshwater and more specifically seawater samples can require pre-concentration and matrix removal in order to increase detection limits, lower the ionic charge in the plasma, or limit isobaric and oxide interferences (*i.e.*: Sn, Sb, Ba). The presence of Ba in the sample is critical in the REE multispike method due to isobaric interferences on La and Ce and BaO interferences on Nd, Sm and Gd. We used three different separation protocols, one suitable for freshwater and two suitable for coastal and open ocean seawaters. All sample preparations were performed under ISO 2 conditions in the LEGOS and GET clean rooms. All acids used were in-house double distilled and deionized (DI) water was <18 MΩ.

2.2.1 Freshwater samples. For freshwater samples, we used a single offline chromatography column using the AG50W-X8 (Dowex) cationic resin.[43] A 200 mm height and 2.5 mm inner diameter quartz column equipped with a 1 mm frit is filled with 100–200 mesh AG50W-X8 resin. The exchange capacity of the column is approximately of 2.6 meq. The sample is aliquoted and evaporated to dryness, and then dissolved in 2 ml of 2 M HCl, and loaded on the preconditioned column. After a 3 time 200 μl rinse with 2 M HCl, 1.4 ml of 2 M HCl is added to the column followed by 8.2 ml of 2.5 M HNO_3 for Ba removal. The REEs are then eluted in 15 ml of 6 M HCl. A chromatogram of this separation method is shown in Fig. 4. After each sample elution, the column is washed and regenerated with 7 ml of 2.5 M HNO_3 and 20 ml of 6 M HCl. The sample is evaporated to dryness and redissolved in 0.32 M HNO_3 for analysis by SF-ICP-MS. This separation protocol displays a more than 90% recovery even for Lu which is the first REE eluted after Ba and La which is the last REE eluted at the end of the 6 M HCl fraction.

2.2.2 Seawater samples. For seawater samples two pre-concentration protocols were used. The first is inspired by the routine protocol used at the LEGOS laboratory and consists in REE $Fe(OH)_3$ co-precipitation followed by Fe removal with anionic chromatography.[29] The second protocol consists in the retention of REEs onto the Hitachi Nobias™ resin. Both methods are followed by a chromatographic separation step as described in the previous section to ensure a complete removal of Ba.

(a) Fe oxide REE co-precipitation + AG50W-X8 cationic column. REE pre-concentration by co-precipitation with $Fe(OH)_3$ is achieved by adding 0.5 g of purified and HCl dissolved Fe to 100–500 ml of the seawater sample. After 24 h (at least)

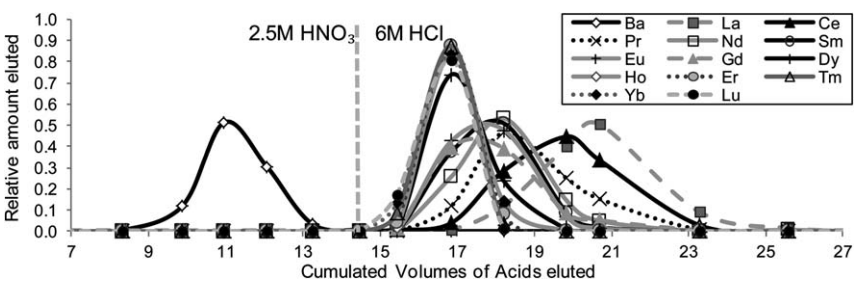

Fig. 4 Ba/REE separation chromatogram with cationic resin AG50W-X8. Volumes are expressed in ml.

homogenization, the pH is increased to 7–8 by addition of ultrapure NH_4OH leading to the formation of an $Fe(OH)_3$ precipitate. After 24 h sedimentation, the precipitate is rinsed and centrifuged 3 times with DI water in order to remove a maximum of water soluble salts. After the last centrifugation step, the sample is evaporated to dryness, the precipitate is dissolved in 6 M HCl and the Fe is separated from the REEs by retention in a 100 mm height and 2.5 mm inner diameter quartz column with a 1 mm frit that is filled with a 200–400 mesh AG1-X8 (Biorad) resin. The REEs are eluted in 6 M HCl and Fe is finally eluted from the column with 0.1 M HCl. This separation protocol usually displays recoveries of REEs superior to 95%; further details can be found in ref. 29. The eluate containing REEs, traces of Ba and other impurities is then evaporated to dryness, redissolved in 2 ml of 2 M HCl, and loaded in the AG50W-X8 cationic column as described in the previous section for Ba separation.

(b) Hitachi Nobias resin + AG50W-X8 cationic column. The Nobias™ PA1 columns (Hitachi High Tech, Japan) are packed with a hydrophilic methacrylate polymer on which ethylenediaminetriacetic and iminodiacetic acids are immobilized that display a very high affinity for trace metals.[44,45] The performance of the Nobias resin was tested for the REE pre-concentration/separation and displayed high recovery of REEs, and very efficient separation of Ba.[32–34]

The Nobias pre-concentration procedure presented in this study was adapted from the previously published studies and involves three steps: washing, pre-concentration and elution. The pre-concentration setup used with the Nobias resin is shown in ESI.† The washing solutions, sample and elution solutions are pumped with a peristaltic pump and a combination of Tygon and Teflon tubing.

The columns are first washed with 10 ml of commercial acetone, followed by 3 ml of DI water and then, 3 ml of 3 M HNO_3. The H_2O/HNO_3 sequence is repeated 3 times to assure the removal of impurities brought by the acetone. For the pre-concentration, the pH of the samples previously filtered and acidified is adjusted to a value of 6 ± 0.2. Therefore a stock of a 2.5 M ammonium acetate buffer solution is prepared with glacial acetic acid (ULTREX II, J.T.Baker®) ammoniac in excess (Merck Suprapur 25%) and DI water. The buffer is added to the sample in order to reach a concentration of 0.125 M and a buffered pH of approximately 4; pH is then secondary raised with ammoniac (Merck Suprapur 25%). Before and after every buffered sample elution, 10 ml of a 0.125 M ammonium acetate buffer in DI at pH 6 are systematically passed through the system for column conditioning.

During washing and pre-concentration, a Tygon tube is connected to the bottom of the column and wastes are pumped with fluxes of 10 ml min^{-1}. In the elution step, the REEs are eluted with 3 ml of 3 M HNO_3; columns are therefore installed on a rack for gravity elution directly into savillex beakers. After elution, columns are ready for re-use. The Nobias resin used in the procedure detailed here displays recoveries of REEs superior to 90%. Eluted samples are then evaporated, redissolved in 2 M HCl and loaded on an AG50W-x8 cationic column as described previously for Ba separation.

2.3 Instrumental parameters

Following the above outlined sample pre-treatment, REE multispike ID measurements were made by SF-ICP-MS (Element-XR, Thermo-Fisher Scientific), operated in low resolution mode with a desolvation nebulization introduction system. Comparative tests were performed on two desolvation systems: the APEX-Q (ESI Inc.) with no N_2 additional gas and the Aridus II (Cetac Inc.) with N_2 as an additional gas. The Aridus II system was kept for this method because it displayed lower oxide formation.

All atomic masses between 135 and 178 plus 129 and 131 were analyzed. This allowed the measurement of all isotopes used for ID, oxide and isobaric interference corrections. For isotopic ratio measuring purpose we opted like Willbold *et al.* (2005) for an acquisition method consisting of repeated fast scan measurements of all isotopes instead of long individual measurements for each isotope. This reduces the time interval between two acquisitions and is less sensitive to small instabilities in the signal due to variation of the sample flow in the introduction system. 60 consecutive sweeps were thus programmed with 4 short measurements per isotope mass made on flat peak tops in low resolution mode. The dwell time per isotope lasted between 0.004 and 0.4 s according to the signal intensity of each isotope in order to increase precision on the least abundant isotopes for a total acquisition time of 6 min per sample.

Isotope measurements with the Element XR SF-ICP-MS are achieved by setting the magnet to the first isotopic mass position. The isotopes to be measured above the magnet mass are reached with electric scans until reaching a default value of 15% mass variation. The magnetic field is then switched to the next mass position followed by a settling time of a few tens of ms. For our method and starting from ^{129}Xe, a 15% mass variation leads to a first magnet jump at mass 149 and a second at mass 171. The magnet jump leads to an unusual instrumental mass bias for the $^{147}Sm/^{149}Sm$ and $^{171}Yb/^{172}Yb$ ratios of up to 10%. The default mass scanning range was therefore modified to a value of 20%. All isotopes between masses 129 and 178 were then covered with a single "magnet jump" at mass 154 and two series of electric scans (135 → 153, and 154 → 178). Setting the "magnet jump" at mass 154 has the advantage of affecting neither the pairs of isotopes used in ID calculation nor the isotopes used for isobaric corrections. Instrument parameters are reported in the ESI.†

2.4 Data treatment

(a) Sequence. A sequence is composed of spiked samples, procedural blanks and CRMs that are regularly bracketed by HNO_3 blanks, monitoring solutions and spike solutions for mass bias and oxide formation corrections.

(b) Blank correction. The first step in the data treatment is the blank correction. Signals on the chemistry blanks (which include the instrumental 0.32 M HNO_3 blank) are typically low (<1%) and directly subtracted from sample signals for most isotope masses. For a better precision of isobaric corrections on La, Ce and Lu (*cf.* paragraph d), Xe, Ba and Hf are not corrected

for blank contribution, and Ce and Yb blank corrections are made after their isobaric interference corrections on La and Lu respectively.

(c) Oxide interference corrections. In the multispike method oxide formation is monitored in two synthetic REE solutions bracketing a series of 5 samples. The first solution contains Ba, La, Ce, Pr, Tb, Er and Yb of natural isotopic composition and allows the monitoring of the following oxides:

$$\%\mathrm{BaO} = {}^{138}\mathrm{Ba}{}^{16}\mathrm{O}/{}^{138}\mathrm{Ba}; \quad (5)$$

$$\%\mathrm{LaO} = {}^{139}\mathrm{La}{}^{16}\mathrm{O}/{}^{139}\mathrm{La}; \quad (6)$$

$$\%\mathrm{CeO} = {}^{140}\mathrm{Ce}{}^{16}\mathrm{O}/{}^{140}\mathrm{Ce}; \quad (7)$$

$$\%\mathrm{PrO} = {}^{141}\mathrm{Pr}{}^{16}\mathrm{O}/{}^{141}\mathrm{Pr}; \quad (8)$$

$$\%\mathrm{TbO} = {}^{159}\mathrm{Tb}{}^{16}\mathrm{O}/{}^{159}\mathrm{Tb}. \quad (9)$$

The second solution contains Nd, Sm, Eu, Gd, and Dy, and allows the monitoring of:

$$\%\mathrm{NdO} = {}^{146}\mathrm{Nd}{}^{16}\mathrm{O}/{}^{146}\mathrm{Nd}; \quad (10)$$

$$\%\mathrm{SmO} = {}^{149}\mathrm{Sm}{}^{16}\mathrm{O}/{}^{149}\mathrm{Sm}; \quad (11)$$

$$\%\mathrm{EuO} = {}^{153}\mathrm{Eu}{}^{16}\mathrm{O}/{}^{153}\mathrm{Eu}; \quad (12)$$

$$\%\mathrm{GdO} = {}^{155}\mathrm{Gd}{}^{16}\mathrm{O}/{}^{155}\mathrm{Gd}; \quad (13)$$

$$\%\mathrm{DyO} = {}^{161}\mathrm{Dy}{}^{16}\mathrm{O}/{}^{161}\mathrm{Dy}. \quad (14)$$

An average value of each elemental oxide formation rate is calculated for the session; the regular analysis of those oxide formation rates allows us to correct with more accuracy the interfering oxides and to monitor their stability. Hydroxide formation was found to be below the detection limit and is therefore not considered in this study.

(d) Isobaric interference corrections. ^{136}Ce, ^{138}La and ^{176}Lu are required for the Ce, La and Yb isotope dilution calculation. These isotopes are respectively interfered by ^{136}Xe and ^{136}Ba, ^{138}Ba and ^{138}Ce and ^{176}Yb and ^{176}Hf. The interference correction of ^{136}Ba and ^{136}Xe on ^{136}Ce is made using the interference free ^{137}Ba and ^{134}Xe isotopes. The correction of ^{138}Ba and ^{176}Hf isobars (on ^{138}La and ^{176}Lu respectively) follows the same logic. The interference correction is less trivial for ^{138}Ce and ^{176}Yb on ^{138}La and ^{176}Lu, because ^{138}Ce and ^{176}Yb are naturally present in the sample and are also added to the mixed spike solutions. The pairs of ratios ^{138}Ce/^{140}Ce *vs.* ^{136}Ce/^{140}Ce and ^{176}Yb/^{171}Yb *vs.* ^{176}Yb/^{172}Yb evolve linearly within the mixing between spike and sample endmembers of contrasted isotopic compositions. These relations allow us to efficiently unravel the combined spike and natural ^{138}Ce and ^{176}Yb contributions to the measured signals on masses 138 and 176. The isobaric corrections are calculated as follows:

$$\mathrm{Cps}^{138}\mathrm{La} = \mathrm{Cps}^{138} - \frac{\mathrm{Cps}^{137}\mathrm{Ba}}{A^{137}\mathrm{Ba}} A^{138}\mathrm{Ba} - \left(\mathrm{Cps}^{136}\mathrm{Ce}0.0305 + 0.0028\mathrm{Cps}^{140}\mathrm{Ce}\right) \quad (15)$$

$$\mathrm{Cps}^{176}\mathrm{Lu} = \mathrm{Cps}^{176} - \frac{\mathrm{Cps}^{177}\mathrm{Hf}}{A^{177}\mathrm{Hf}} A^{176}\mathrm{Hf} - \left(\mathrm{Cps}^{171}\mathrm{Yb}0.909 + 0.0101\mathrm{Cps}^{172}\mathrm{Yb}\right) \quad (16)$$

where Cps^{138} is the measured total ion count on mass 138, '*A*' refers to natural abundance, and coefficients '0.0305 and 0.0028' are the slope and intercepts of the mixing diagrams (idem for Lu). Note that in addition mass bias corrections are made to eqn (15) and (16) (see next section).

(e) Mass bias correction. Isotopic ratios used for isotope dilution and isobaric corrections are corrected for instrumental mass bias, with a fractionation factor calculated as follows:

$$f_{x/y} = \frac{\left(\frac{\mathrm{Cps}^x M}{\mathrm{Cps}^y M}\right)}{\left(\frac{A^x M_{\mathrm{nat}}}{A^y M_{\mathrm{nat}}}\right)} \quad (17)$$

$f_{x/y}$: fractionation factor between the *M* REE pair of isotopes of *x* and *y* masses.

$\mathrm{Cps}^x M$: counts per second of the *M* REE isotope of *x* mass.

$A^x M_{\mathrm{nat}}$: natural abundance of the *M* REE isotope of *x* mass.

Fractionation factors are calculated from the same analysis of the synthetic bracketing solutions that are also used for determining oxide formation (Ba, La, Ce, Pr, Tb, Er, Yb and Nd, Sm, Eu, Gd, Dy). A series of 5 samples are bracketed with monitoring solutions and blanks. For each series, an average fractionation factor is calculated using the two bracketing analyses. The factor is then applied to correct for mass bias on samples as follows.

$${}_{\mathrm{corr}}R_{x/y} = \frac{\left(\frac{\mathrm{Cps}^x M_{\mathrm{smp}}}{\mathrm{Cps}^y M_{\mathrm{smp}}}\right)}{f^i_{x/y}} \quad (18)$$

The ^{131}Xe/^{136}Xe mass bias is also monitored in the 0.32 M HNO3 instrument blank solution after corrections from minor ^{136}Ce and ^{136}Ba isobaric interferences. Due to low signals and highly interfered natural ^{138}La, ^{136}Ce and ^{175}Lu in the bracketing monitoring solutions, mass bias for ^{138}La/^{139}La, ^{136}La/^{140}La and ^{175}Lu/^{176}Lu is monitored in the 'mixed spike' solutions which display sufficient ^{138}La, ^{136}Ce and ^{175}Lu signals.

(f) Mono-isotopic REEs. The mono-isotopic REE (*i.e.*: Pr, Tb, Ho, Tm) concentrations are determined by external calculation using a bracketing standard and are corrected for chemistry yields using isotope diluted REEs as internal standards. This method readily integrates the dilution factor, preparation chemistry yields and avoids the need of a third internal standard sometimes used in concentration determination (*i.e.* Tm, In or Re) to correct the shift of sensitivity between standard and sample. This shift of sensitivity is commonly due to the time elapsed between the two measurements and differences of matrix compositions or little variation of the sample flow in the introduction system. Ratios between sample concentrations obtained by isotope dilution and externally calculated concentrations are monitored for ^{143}Nd, ^{145}Nd, ^{146}Nd, ^{147}Sm, ^{149}Sm, ^{151}Eu, ^{153}Eu, ^{155}Gd, ^{157}Gd, ^{161}Dy, ^{163}Dy, ^{166}Er, ^{167}Er, ^{171}Yb and ^{172}Yb.

As illustrated for ^{151}Eu:

$$R_{\frac{^{151}\mathrm{Eu_{smp}}}{^{151}\mathrm{Eu_{bk}}}} = \frac{\left([^{151}\mathrm{Eu}]_{\mathrm{ID}} + [^{151}\mathrm{Eu}]_{\mathrm{spk}}\right)}{[^{151}\mathrm{Eu}]_{\mathrm{EC}}} \quad (19)$$

Abbreviations smp and bk stand for sample and beaker.

Abbreviations ID and EC stand for the isotope concentration determined by "isotope dilution" and "calculated externally". Spk stands for the spike isotope concentration.

$$R_{\frac{^{151}\mathrm{Eu_{smp}}}{^{151}\mathrm{Eu_{bk}}}} = \frac{\left([\mathrm{Eu}]_{\mathrm{ID}} A^{151}\mathrm{Eu_{nat}} + \frac{\left(W_{\mathrm{s}}[\mathrm{Eu}]_{\mathrm{LREEspk}} A^{151}\mathrm{Eu_{spk}}\right)}{W_{\mathrm{e}}}\right)}{\frac{[\mathrm{Eu}]_{\mathrm{std}}\, A^{151}\mathrm{Eu_{nat}}}{\mathrm{Cps}^{151}\mathrm{Eu_{std}}\mathrm{Cps}^{151}\mathrm{Eu_{sap}}}} \quad (20)$$

LREEspk: "mixed LREE spike".

'nat' and 'std' stand for natural and standard.

An average $R_{\mathrm{smp/bk}}$ is then calculated for each element, and a linear regression is then fitted between individual elemental R and the corresponding atomic masses. The $R_{\mathrm{smp/bk}}$ are then inferred for Pr, Tb, Tm and Ho masses and multiplied by their externally calculated concentrations.

3 Results and discussion

In this section we discuss: (1) the performance of the multispike SF-ICP-MS method, and (2) results for certified reference materials SLRS-4 and SLRS-5 river water and CASS-5 coastal seawater. We also compare open ocean samples collected during a GEOTRACES intercalibration cruise at the BATS (Bermuda Atlantic Time Series) station at depths of 15 m (GS63) and 2000 m (GD41).

3.1 Separation chemistry

The most critical aspect of the separation chemistry is the removal of Ba. ^{136}Ba and ^{138}Ba interfere with spike isotopes ^{136}Ce and ^{138}La respectively. We discuss here the case of ^{138}Ba. Due to the lower La concentration in seawater than in river water, the Ba/La ratio is typically more elevated in seawater. The efficiency of Ba removal during the sample processing was evaluated from the $(^{138}\mathrm{Ba}/^{138}\mathrm{La})_{\mathrm{nat}}$ and $(^{138}\mathrm{Ba}/(^{138}\mathrm{La_{nat}} + {}^{138}\mathrm{La_{spk}}))$ ratios for 7 different samples analyzed in this study and processed with different separation/pre-concentration techniques (Table 2). A co-precipitation step applied to river and seawater samples causes a 50- to 250-fold reduction in the [Ba]/[La] ratio for seawater but does not affect significantly the Ba/La ratio of river water samples. Even with enriched ^{138}La spike addition to the sample, the ^{138}Ba/^{138}La ratios are still too high to perform ID on river water La with a single co-precipitation step.

The ionic exchange capacity of AG50W-X8 is sufficient to process a river water sample and remove most of the Ba. SLRS-4 and SLRS-5 show a 2000-fold drop in the Ba level, allowing a La ID calculation with a 25% isobaric correction of ^{138}Ba on ^{138}La. However, this method is not powerful enough for seawater samples.

The combination of the $Fe(OH)_3$ co-precipitation + AG1X-8 and the AG50W-X8 cationic exchange chromatography resulted in a 15 000- to 40 000-fold removal of Ba for CASS-5 and the GS seawater samples. Only 100 ml of CASS-5 was co-precipitated and a one-fold overspiking was performed for this CRM to limit the Ba blank contribution. This allowed an ID calculation for La with a 50% residual Ba correction.

The Nobias separation protocol achieves a 1300- to 19 000-fold drop in Ba concentration. This is insufficient for La ID as a residual 90% isobaric interference correction on ^{138}La remains. A severe overspiking of La would be necessary to counteract the amount of correction needed. Finally, for seawater samples, the combination of the Nobias and cationic AG50W-X8 displayed the most efficient Ba removal for this study with a minimum of 50 000-fold drop in Ba levels.

In this study we therefore adopted both Nobias + AG50W-X8 or Fe co-precipitation + AG1-X8 + AG50W-X8 protocols for seawater. For river waters we used exclusively the single pass AG50W-X8 protocol. Final ^{138}Ba corrections on ^{138}La ranged from 10% to 65%. Final ^{136}Ba corrections on ^{136}Ce ranged from 14% to 66% and ^{176}Hf corrections on ^{176}Lu ranged from 2% to 5%.

3.2 Analysis performance

(a) Sensitivity, blanks. SF-ICP-MS sensitivity, detection and quantification limits, solvent concentration and chemistry

Table 2 Efficiency of pre-concentration/separation protocols for Ba removal. 'Cop.' refers to co-precipitation. AM3 803 and AM3 102 are seawater and river water endmember samples (salinities 36.2 and 0) from the Amazon estuary collected on 4/10/2008 in the framework of the AMANDES project

		Untreated sample		Cop. + AG1-X8		AG50W-X8		Cop. + AG1-X8 + AG50W-X8		Nobias		Nobias + AG50W-X8	
Sample type	Sample id	$\frac{[\mathrm{Ba}]}{[\mathrm{La}]_{\mathrm{nat}}}$	$\frac{^{138}\mathrm{Ba}}{^{138}\mathrm{La}}$ spiked	$\frac{[\mathrm{Ba}]}{[\mathrm{La}]_{\mathrm{nat}}}$	$\frac{^{138}\mathrm{Ba}}{^{138}\mathrm{La}}$ spiked	$\frac{[\mathrm{Ba}]}{[\mathrm{La}]_{\mathrm{nat}}}$	$\frac{^{138}\mathrm{Ba}}{^{138}\mathrm{La}}$ spiked	$\frac{[\mathrm{Ba}]}{[\mathrm{La}]_{\mathrm{nat}}}$	$\frac{^{138}\mathrm{Ba}}{^{138}\mathrm{La}}$ spiked	$\frac{[\mathrm{Ba}]}{[\mathrm{La}]_{\mathrm{nat}}}$	$\frac{^{138}\mathrm{Ba}}{^{138}\mathrm{La}}$ spiked	$\frac{[\mathrm{Ba}]}{[\mathrm{La}]_{\mathrm{nat}}}$	$\frac{^{138}\mathrm{Ba}}{^{138}\mathrm{La}}$ spiked
Seawater	CASS-5	>1000	$>2 \times 10^4$	—	—	—	—	0.06	0.9	—	—	—	—
	GD 41	>2500	$>8 \times 10^4$	43	1330	—	—	—	—	1.8	56	0.06	1.4
	GS 63	>3500	$>9.5 \times 10^4$	13	308	—	—	0.08	2.2	0.18	4.5	0.01	0.18
	AM3 803	>2500	$>10^5$	32	1551	—		—	—	0.56	26	0.005	0.16
River water	SLRS-4	42	1202	—	—	0.023	0.46	—	—	—	—	—	—
	SLRS-5	62	1823	—	—	0.028	0.56	—	—	—	—	—	—
	AM3 102	65	1146	41	713	—	—	—	—	0.77	14	0.025	0.32

Table 3 REE sensitivity (Sens.), detection and quantification limits (LOD, LOQ), at instrumental (0.32 M HNO_3) and procedural blank levels. 'Mcps' stands for 10^6 counts per second

					Chemistry blanks (pg)		
	Sens. (Mcps per ppb)	LOD (ppq)	LOQ (ppq)	0.32 M HNO_3 (ppq)	AG50W-X8	Cop + AG1-X8 + AG50W-X8	Nobias + AG50W-X8
Ba	4.3	30	99	1293	20	27	33
La	4.7	15	50	76	2.3	5	2.9
Ce	4.9	11	37	72	3.3	13	7
Pr	5.3	1	5	22	0.4	0.77	0.51
Nd	5.5	2	5	72	1.05	2.22	1.41
Sm	5.4	3	9	86	0.31	0.42	0.36
Eu	5.6	3	8	32	0.10	0.07	0.14
Gd	5.8	3	9	172	0.28	0.14	0.62
Tb	6.0	2	6	10	0.06	0.06	0.06
Dy	6.3	1	4	37	0.36	0.35	0.39
Ho	6.5	1	4	6	0.06	0.07	0.07
Er	6.6	1	3	24	0.15	0.22	0.19
Tm	6.6	1	4	6	0.07	0.06	0.07
Yb	6.5	1	2	53	0.25	0.37	0.55
Lu	6.6	1	4	12	0.05	0.05	0.08

blanks are reported in Table 3. The typical sensitivity was 5 million ion counts per parts-per-billion (Mcps per ppb) for In and 8 Mcps per ppb for U. REE isotope concentrations in processed samples were adjusted to give maximum signals of 3 Mcps. This assured that all isotopes were measured in ion counting mode, and avoided potential bias from analogous to ion counting mode inter-conversion (>4.5 Mcps).

River waters such as SLRS-4 and SLRS-5 in fact do not need to be pre-concentrated to achieve sufficient sensitivity. However, for the purpose of Ba removal, river waters were processed with final pre-concentration factors from 0.55 to 1.5. For seawater samples, the 200-fold pre-concentration factor that is applied in our lab for REE analysis by Q-ICP-MS was reduced to factors of 16 to 33 for coastal CASS-5 and 25 to 50 for open ocean BATS samples (GD41 and GS63).

The multispike SF-ICP-MS method then permits a full REE analysis of a 50 ml seawater sample. However as procedural blanks are a limiting factor, by precaution samples volumes were kept higher with 100 ml for CASS-5, 250 ml for GD41, and 500 ml for GS63. Instrumental blank signals in 0.32 M HNO_3 were systematically more than 3 orders of magnitude inferior to sample measurement signals. Instrumental detection limits for the REE were in the range of 0.005 to 1 ppq. Overall REE chemistry blanks are <1 pg, except for La, Ce and Nd with the co-precipitation + AG1-X8 + AG50W-X8 and Nobias + AG50W-X8 seawater protocols (<15 pg).

For ^{139}La, chemistry blank corrections were low with 0.08% for SLRS-4 and SLRS-5, 0.29% for CASS-5, 0.4% for GD41 and 0.15% for GS63. For ^{140}Ce blanks were less than 0.12% for SLRS-4 and SLRS-5 processed with AG50W-X8 but reached up to 2% for CASS-5 samples and up to 3% for GD41 and inferior to 0.8% for GS63. Relatively high blank corrections were also observed for ^{155}Gd, ^{169}Tm and ^{159}Tb ranging from 0.6% to 1.7% for the samples analyzed. All other isotopes analyzed had blank corrections <0.4%.

The excellent sensitivity and detection limits obtained with our protocol would allow lowering substantially the initial sample volumes. However, this clearly requires further efforts in order to reduce chemistry blank contributions. For CASS-5, using less than 100 ml would yield significant blank corrections. For the co-precipitation protocol, the chemistry blanks can potentially be reduced by lowering the amount of iron added to the sample and for the Nobias protocol by improving the wash and rinse steps of the column and reducing the amount of buffer added to the sample.

(b) Oxide production. Oxide formation levels of the desolvation–SF-ICP-MS setup were described in the Materials and methods section. The use of the CETAC Aridus II as the introduction system reduces oxide formation down to values inferior to 0.001% for BaO/Ba, 0.0035% for LaO/La and 0.002% for CeO/Ce. At these levels, the corrections induced on interfered isotopes are insignificant and comparable to instrumental 0.32 M HNO_3 blank signals. Maximum corrections of 1.6% and 0.25% were made for ^{139}LaO on ^{155}Gd and ^{149}SmO on ^{165}Ho respectively.

The previously published multispike method for REE analysis in rock materials on a MC-ICP-MS required chromatographic separation of LREEs and HREEs in order to avoid oxide interferences due to enriched LREE patterns in rocks and the significantly higher oxide production when operating the desolvator with no additional gas.[39] It appears that the use of a desolvating introduction system with additional nitrogen gas is an interesting alternative for water samples usually depleted in HREEs.

(c) Isotope dilution. Except for La and Lu, which were overspiked to avoid substantial isobaric interference corrections of ^{138}Ba and ^{138}Ce on ^{138}La and ^{176}Yb and ^{176}Hf on ^{176}Lu, the long-term uncertainty magnification factors of REE concentration analysis by the multispike method, based on the 19 samples presented, were close to the ideal limit.

3.3 Reference solution analysis

(a) Canadian National Research Council reference solutions. SLRS-4 and SLRS-5 river water reference solutions and CASS-5 seawater (CNRC) were analyzed. 5 ml of SLRS-4 and SLRS-5 and 100 ml of CASS-5 were spiked. 5 spiked replicates were prepared and each replicate was analyzed 2 or 3 times during 2 SF-ICP-MS sessions. Details of the sample treatment procedures, concentrations expressed in parts-per-trillion (ppt) and confidence intervals in 2 SD and 2 RSD are reported in Table 4. Although REEs are not certified for these solutions an intercalibration effort was made for SLRS-4 and our results are in good agreement with those published.[46] All REE concentrations are within the 1SD interval as shown in a post-Archean average Australian shale (PAAS) normalized REE diagram[42] (Fig. 5). Most of the REEs analyzed with our method have 2SD confidence intervals inferior to 2% with an exception of La and Tb. This is probably due to the propagation of error in the estimation of ^{138}La isobaric interferants and because REEs before the "peak jump" are used to infer mono-isotopic Tb recovery. For SLRS5, our results are within the 2SD interval of recently published results of SLRS-5 REE concentrations based on the SLRS-4/SLRS-5 ratios.[47]

Like SLRS-4 and SLRS-5, 2RSD confidence intervals for coastal CASS-5 CRM are generally inferior to 2%, except La, Ce, and Nd that display 2RSDs between 3.1% and 4.7%. When normalised to PAAS, CASS-5 REEs display classical seawater fractionation patterns with a gradual enrichment from LREEs to HREEs and a negative Ce anomaly (Fig. 6).

Anomalies were calculated for Ce, Sm, and Gd, with methods described by several authors (Table 5) and by linear regression inspired by Kulaksiz and Bau (2011).[16,48] These authors made a linear least square regression of coherent logarithmic values of PAAS normalised REEs ($\log(REE_{PAAS})$) (Pr, Nd, Sm) against their ranking amongst the lanthanide series (*i.e.* from 1 to 15) for tap water samples in order to infer the Gd background value. We

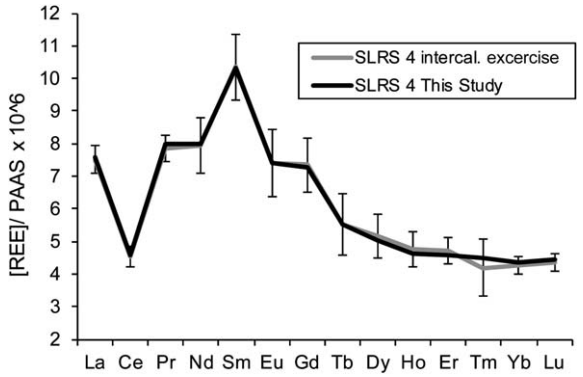

Fig. 5 REE patterns for the SLRS-4 intercalibration effort (grey line) and that measured in this study (black line). REE concentrations expressed in ppt are normalized to PAAS and multiplied by 10^6. 1SD confidence interval for the intercalibration data is shown.

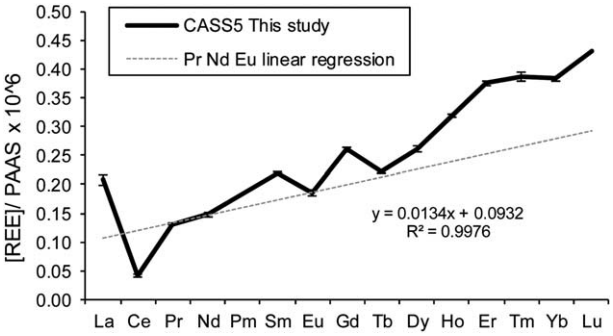

Fig. 6 REE pattern for the coastal seawater CASS-5 measured in this study (black line). REE concentrations expressed in ppt are normalized to PAAS and multiplied by 10^6. The linear regression line between Pr, Nd, Sm, Eu and Dy is reported (grey line). 2SD confidence intervals are reported with error bars.

Table 4 SLRS-4, SLRS-5 and CASS-5 REE analyses of this study, intercalibrated concentrations of the SLRS-4 river water reference solutions (Yeghicheyan *et al.*,[46] 2001)*, and published concentrations of SLRS-5 (Heimburger *et al.*,[47] 2012)**. SLRS-4 and SLRS-5 were processed with AG50W-X8 and CASS-5 with co-precipitation + AG1-X8 + AG50W-X8

	SLRS-4*		SLRS-4, this study			SLRS-5**		SLRS-5, this study			CASS-5, this study		
	ppt ($n = 5$) 174 anal.	2SD	ppt ($n = 10$)	2SD	2RSD	ppt	2SD	ppt ($n = 11$)	2SD	2RSD	ppt ($n = 11$)	2SD	2RSD
La	287.0	16.1	290.3	12.8	4.4%	196	44	213.6	9.25	4.3%	7.95	0.35	4.5%
Ce	360.0	24.5	364.1	6.94	1.8%	236	32	254.8	6.11	2.4%	3.36	0.16	4.7%
Pr	69.3	3.60	70.6	4.59	1.6%	46.9	5.0	50.33	1.19	2.4%	1.163	0.014	1.2%
Nd	269.0	28.5	270.3	5.54	1.5%	185	40	197.1	4.58	2.3%	5.02	0.16	3.1%
Sm	57.4	5.63	57.2	0.62	1.2%	32.4	6.6	33.11	0.19	0.6%	1.215	0.008	0.7%
Eu	8.00	1.10	8.00	0.13	1.9%	5.6	2.8	5.88	0.09	1.6%	0.201	0.003	1.7%
Gd	34.2	3.90	33.8	0.72	2.1%	24.9	6	26.08	0.62	2.4%	1.211	0.026	2.2%
Tb	4.3	0.72	4.30	0.23	4.2%	3.2	1.2	3.43	0.11	3.2%	0.173	0.004	2.1%
Dy	24.2	3.10	23.6	0.32	1.4%	18.2	5	18.89	0.22	1.1%	1.226	0.012	1.0%
Ho	4.7	0.54	4.60	0.36	1.1%	3.6	1	3.65	0.05	1.4%	0.315	0.005	1.6%
Er	13.4	1.21	13.1	0.12	0.9%	10.5	2	10.63	0.09	0.8%	1.066	0.008	0.8%
Tm	1.7	0.35	1.80	0.03	1.7%	1.3	0.6	1.49	0.02	1.2%	0.157	0.002	1.3%
Yb	12.00	0.77	12.3	0.14	1.2%	9.3	1.4	10.13	0.15	1.4%	1.084	0.010	0.9%
Lu	1.9	0.12	1.95	0.03	1.4%	1.5	0.4	1.64	0.02	1.5%	0.189	0.004	1.9%

Table 5 Definitions and values of REE anomalies discussed in the text for the CASS-5 coastal seawater CRM. * refers to the background value of the anomalous REE and pn refers to PASS normalised

Equation	Reference	Anomaly	2RSD
$Ce_{pn}/Ce^* = Ce_{pn}/(2Pr_{pn} - Nd_{pn})$	(Bolhar *et al.*, 2004)[53]	0.371	6.1%
$Ce_{pn}/Ce^* = Ce_{pn}/f(Pr_{pn}, Nd_{pn}, Eu_{pn})$	—	0.355	4.8%
$Sm_{pn}/Sm^* = 3Sm_{pn}/(Nd_{pn} + 2Eu_{pn})$	(Alibo and Nozaki, 1999)[30]	1.264	1.7%
$Sm_{pn}/Sm^* = Sm_{pn}/f(Pr_{pn}, Nd_{pn}, Eu_{pn})$	—	1.266	1.6%
$Gd_{pn}/Gd^* = 2Gd_{pn}/(Eu_{pn} + Tb_{pn})$	(De Baar *et al.*, 1985)[54]	1.282	2.3%
$Gd_{pn}/Gd^* = Gd_{pn}/f(Pr_{pn}, Nd_{pn}, Eu_{pn})$	—	1.309	2.1%

used Pr, Nd and Eu PAAS normalised concentrations for the linear regression (without logarithm) as illustrated in Fig. 6 (Pm was introduced in the lanthanide diagram to show the coherent Pr, Nd and Eu normalised patterns as a function of their ranking).

REE anomalies were calculated for each replicate analysis in order to be able to calculate average values and associated 2RSD. All anomalies calculated by alternative equations show the same value within the associated confidence intervals. Besides the typical seawater Ce anomaly in CASS-5, three major additional anomalies can be observed for La, Sm and Gd. The unusual Sm anomaly was also observed on other CNRC CRMs like SLRS-4 and SLRS-5 (this study), CASS-4 and NASS-5 and has been attributed to Sm contamination during CRM preparation.[49–51] With the exception of Ce, the anomalies calculated for CASS-5 replicates display low uncertainties of 1.7% 2RSD (Sm) and 2.2% 2RSD (Gd). Ce anomalies present 2RSD uncertainties of 4.8% and 6.1% due to the higher uncertainties of La and Ce concentrations. Nevertheless our uncertainty on the Ce anomaly is inferior to the typical 9–21% 2RSD uncertainties calculated for the recent GEOTRACES seawater REE intercomparison.[38]

(b) BATS station GEOTRACES intercalibration. Dedicated REE samples collected during a GEOTRACES intercalibration cruise were completely consumed after the analysis by 9 laboratories.[38,52] K. Bruland kindly provided us with closely related samples from the same station and depths, yet preserved for other trace metal intercalibration efforts. We received 500 ml aliquots of filtered (0.2 μm) acidified seawater stored in HDPE bottles.

For the GD41 BATS 2000 m deep water sample two 250 ml sub-aliquots were made and spiked independently. For the GS63 BATS 15 m surface water sample 500 ml was spiked. In an initial attempt, the samples were passed through the Nobias column and analysed twice to determine all REE concentrations except La and Ce which had >90% interferences from Ba isotopes. To lower Ba interferences, the remaining sample was passed through the AG50W-X8 column, allowing more accurate and precise La and Ce concentration determination in a third analysis session.

Table 6 reports REE concentrations published by the GEOTRACES intercalibration effort and GD41 and GS63 REE concentrations determined in this study. Concentrations are expressed in ppt, confidence intervals in 2SD and 2 RSD%. For both GD41 and GS63 all REEs are within the 2SD confidence interval established during the intercalibration exercise (Fig. 7a and b). The BATS surface and deep samples reveal numerous subtle REE features: Ce anomalies calculated according to Bolhar *et al.* (2004)[53] increase from 0.177 at 15 m to 0.518 at 2000 m depth. Well-developed Gd anomalies for Atlantic

Table 6 Intercalibrated REE concentrations of the 2000 m and 15 m (Van de Flierdt *et al.*, 2012) waters from North East Atlantic BATS station, and corresponding GD41 and GS63 samples analysed in this study (samples were treated with Nobias + AG50W-X8)

	BATS 2000 m intercalibration		BATS 2000 m GD41, this study			BATS 15 m intercalibration		BATS 15 m GS63, this study
	ppt	2SD	ppt	2SD	2RSD	ppt	2SD	ppt
La	3.28	0.39	3.25	—	—	2.05	0.31	2.16
Ce	0.72	0.328	0.72	—	—	1.68	0.38	1.64
Pr	0.568	0.050	0.556	0.011	2.4%	0.439	0.052	0.439
Nd	2.49	0.18	2.53	0.02	0.7%	2.04	0.19	2.00
Sm	0.519	0.051	0.505	0.005	1.1%	0.482	0.054	0.464
Eu	0.138	0.015	0.131	0.003	2.0%	0.135	0.016	0.130
Gd	0.761	0.083	0.757	0.013	1.8%	0.760	0.086	0.759
Tb	0.125	0.012	0.116	0.002	1.4%	0.126	0.013	0.122
Dy	0.943	0.062	0.916	0.004	0.4%	0.959	0.085	0.948
Ho	0.251	0.015	0.237	0.003	0.8%	0.245	0.022	0.243
Er	0.843	0.042	0.814	0.005	0.8%	0.803	0.071	0.808
Tm	0.126	0.008	0.119	0.001	0.8%	0.118	0.011	0.113
Yb	0.824	0.043	0.814	0.018	2.2%	0.719	0.089	0.734
Lu	0.141	0.007	0.141	0.004	2.3%	0.117	0.016	0.122

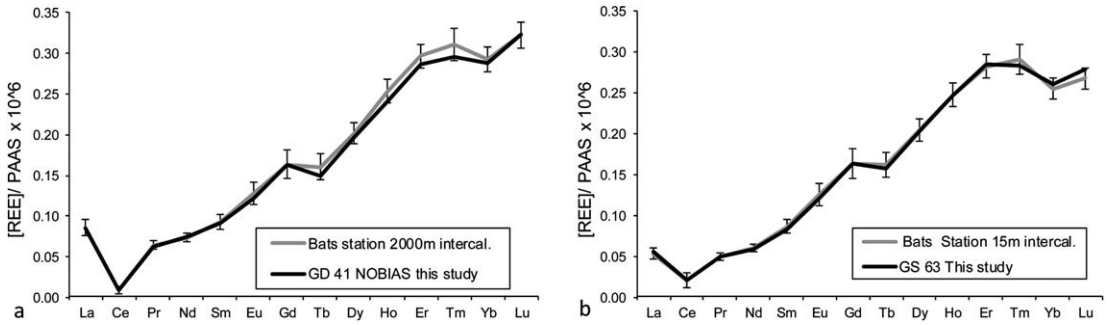

Fig. 7 REE patterns for the intercalibrated BATS station at depths (a) 15 m and (b) 2000 m (Van de Flierdt *et al.*, 2012)[38] (grey lines) and the corresponding (a) GD41 and (b) GS63 samples (black lines, this study). REE concentrations expressed in ppt are normalized to PAAS and multiplied by 10^6. 2SD confidence intervals for the intercalibration data are shown.

samples are present, and are constant at both depths, in agreement with observations in the literature.[11,14,38] HREEs Yb and Lu are significantly fractionated between both depths. Finally, La also appears fractionated between both depths with La_{pn}/Ce_{pn} ratios of 1.14 on the surface and 1.35 at 2000 m. All of these features reflect the interplay between input sources and elemental fractionation processes related to REE speciation.

4 Conclusions

Based on existing methodologies and technologies we have developed a high precision method for the analysis of REEs in fresh and marine waters. The method is based on multiple isotope dilution of 10 out of 14 stable REEs, followed by pre-concentration and matrix removal using Fe co-precipitation and/or ion chromatography. By using a desolvation introduction system to a sector field ICP-MS, we achieve maximum sensitivity and minimize polyatomic oxide interferences of Ba and LREEs on HREEs. With oxide formation below 0.035% (LaO^+/La^+), polyatomic oxide interference corrections are below 2% for all REEs. The long term analytical reproducibility is <2% (2RSD) on all REEs, except La (4.5%) and Ce (4.7%), which are limited by blank and interference corrections. Mono-isotopic REEs are also reproducible to better than 4.2% (2RSD) using spiked REEs as internal standards. These results are superior to most ICP-MS based REE analysis methods for natural waters.[38]

While the separation chemistry protocols and data treatment are not trivial, the method does present an interesting compromise to gather high precision REE data on large numbers of aqueous samples with a moderate time investment. Two chemistry protocols were tested for seawater samples. The protocol including the new Nobias resin allows a better Ba removal and a faster sample preparation compared to the traditional $Fe(OH)_3$ co-precipitation. By using two mixed LREE and HREE spike solutions the method provides the flexibility to cover a range of REE profiles, *i.e.* LREE or HREE enriched, or concave or convex MREE enriched. Further improvements are possible for Ce by improving blanks, and the use of a different enriched Ce isotope spike as ^{136}Ce used in this study is heavily interfered by ^{136}Ba and ^{136}Xe. We anticipate that the strong gain in precision on REE patterns and anomalies will stimulate experimental and natural observations on the REE aqueous geochemistry.

Acknowledgements

We would like to thank the following agencies and colleagues: The French CNRS and Brazilian CNPq for funding the 1st author's PhD scholarship. Research grant ANR-05-BLAN-0179 from the French ANR. FEDER, CNRS-INSU, IRD and OMP for funding the OMP mass spectrometry facilities. C. Pradoux, E. Garcia, J. Riotte, M. Benoit, D. Yeghicheyan, L. Laffont, and P. Brunet for valuable discussions. K Bruland for providing GEOTRACES BATS inter-calibration samples. Hitachi for providing the Nobias resin. The two anonymous reviewers and editor are thanked for their constructive comments.

Notes and references

1 G. N. Hanson, *Annu. Rev. Earth Planet Sci.*, 1980, **8**, 371–406.
2 R. A. Stern and G. N. Hanson, *J. Petrol.*, 1991, **32**, 201–238.
3 S. M. Lev, S. M. McLennan and G. N. Hanson, *J. Sediment. Res.*, 1999, **69**, 1071–1082.
4 P. Henderson, *Rare earth element geochemistry*, Elsevier, Amsterdam, New York, 1984, p. 510.
5 K. Tachikawa, C. Handel and B. Dupré, *Deep Sea Res. Oceanogr. Res. Paper*, 1997, **44**, 1769–1792.
6 M. Bau, P. Möller and P. Dulski, *Mar. Chem.*, 1997, **56**, 123–131.
7 E. Sholkovitz and R. Szymczak, *Earth Planet. Sci. Lett.*, 2000, **179**, 299–309.
8 D. J. Piepgras and S. B. Jacobsen, *Geochim. Cosmochim. Acta*, 1992, **56**, 1851–1862.
9 H. Elderfield, R. Upstill-Goddard and E. R. Sholkovitz, *Geochim. Cosmochim. Acta*, 1990, **54**, 971–991.
10 K. H. Johannesson, K. J. Stetzenbach and V. F. Hodge, *Geochim. Cosmochim. Acta*, 1997, **61**, 3605–3618.
11 F. Lacan and C. Jeandel, *Geochem., Geophys., Geosyst.*, 2004, **5**(11), DOI: 10.1029/2004gc000742.
12 R. E. Hannigan and E. R. Sholkovitz, *Chem. Geol.*, 2001, **175**, 495–508.
13 A. Masuda and Y. Ikeuchi, *Geochem. J.*, 1979, **13**, 19–22.

14 H. J. W. De Baar, P. G. Brewer and M. P. Bacon, *Geochim. Cosmochim. Acta*, 1985, **49**, 1961–1969.
15 S. Kulaksiz and M. Bau, *Environ. Int.*, 2011, **37**, 973–979.
16 S. Kulaksiz and M. Bau, *Appl. Geochem.*, 2011, **26**, 1877–1885.
17 S. M. McLennan, *Geochim. Cosmochim. Acta*, 1994, **58**, 2025–2033.
18 M. F. Thirlwall, *Chem. Geol.*, 1982, **35**, 155–166.
19 J. G. Crock, F. E. Lichte and T. R. Wildeman, *Chem. Geol.*, 1984, **45**, 149–163.
20 P. J. Hooker, R. K. O'Nions and R. J. Pankhurst, *Chem. Geol.*, 1975, **16**, 189–196.
21 B.-M. Jahn, B. Auvray, S. Blais, R. Capdevila, J. Cornichet, F. Vidal and J. Hameurt, *J. Petrol.*, 1980, 201–244.
22 J. J. Braun, J. Viers, B. Dupre, M. Polve, J. Ndam and J. P. Muller, *Geochim. Cosmochim. Acta*, 1998, **62**, 273–299.
23 K. H. Johannesson, I. M. Farnham, C. X. Guo and K. J. Stetzenbach, *Geochim. Cosmochim. Acta*, 1999, **63**, 2697–2708.
24 C. H. Gammons, S. A. Wood and D. A. Nimick, *Geochim. Cosmochim. Acta*, 2005, **69**, 3747–3758.
25 J. Ingri, A. Widerlund, M. Land, O. Gustafsson, P. Andersson and B. Ohlander, *Chem. Geol.*, 2000, **166**, 23–45.
26 C. H. Chung, I. Brenner and C. F. You, *Spectrochim. Acta, Part B*, 2009, **64**, 849–856.
27 M. G. Lawrence, A. Greig, K. D. Collerson and B. S. Kamber, *Appl. Geochem.*, 2006, **21**, 839–848.
28 S. J. Goldstein and S. B. Jacobsen, *Earth Planet. Sci. Lett.*, 1988, **89**, 35–47.
29 F. Lacan and C. Jeandel, *Earth Planet. Sci. Lett.*, 2001, **186**, 497–512.
30 D. S. Alibo and Y. Nozaki, *Geochim. Cosmochim. Acta*, 1999, **63**, 363–372.
31 M. B. Shabani, T. Akagi and A. Masuda, *Anal. Chem.*, 1992, **64**, 737–743.
32 P. O. Persson, P. S. Andersson, J. Zhang and D. Porcelli, *Anal. Chem.*, 2011, **83**, 1336–1341.
33 H. Takata, K. Tagami, T. Aono and S. Uchlida, *At. Spectrosc.*, 2009, **30**, 10–19.
34 Y. Zhu, T. Umemura, H. Haraguchi, K. Inagaki and K. Chiba, *Talanta*, 2009, 891–895.
35 G. Bayon, D. Birot, C. Bollinger and J. A. Barrat, *Geostand. Geoanal. Res.*, 2010, **35**, 145–153.
36 J. Zhang and Y. Nozaki, *Geochim. Cosmochim. Acta*, 1996, **60**, 4631–4644.
37 M. P. Field and R. M. Sherrell, *Anal. Chem.*, 1998, **70**, 4480–4486.
38 T. Van de Flierdt, K. Pahnke, H. Amakawa, P. Andersson, C. Basak, B. Coles, C. Colin, K. Crocket, M. Frank, N. Frank, S. L. Goldstein, V. Goswami, B. A. Haley, E. C. Hathorne, S. R. Hemming, G. M. Henderson, C. Jeandel, K. Jones, K. Kreissig, F. Lacan, M. Lambelet, E. E. Martin, D. R. Newkirk, H. Obata, L. Pena, A. M. Piotrowski, C. Pradoux, H. D. Scher, H. Schoberg, S. K. Singh, T. Stichel, H. Tazoe, D. Vance, J. J. Yang and G. I. Partici, *Limnol. Oceanogr.: Methods*, 2012, **10**, 234–251.
39 J. Baker, T. Waight and D. Ulfbeck, *Geochim. Cosmochim. Acta*, 2002, **66**, 3635–3646.
40 M. Willbold, K. Jochum, I. Raczek, M. Amini, B. Stoll and A. Hofmann, *Anal. Bioanal. Chem.*, 2003, **377**, 117–125.
41 M. Willbold and K. P. Jochum, *Geostand. Geoanal. Res.*, 2005, **29**, 63–82.
42 S. McLennan, *Rev. Mineral. Geochem.*, 1989, 169–200.
43 G. C. Martin, *J. Inorg. Nucl. Chem.*, 1964, **26**, 1621–1623.
44 D. V. Biller and K. W. Bruland, *Mar. Chem.*, 2012, **130**, 12–20.
45 Y. Sohrin, S. Urushihara, S. Nakatsuka, T. Kono, E. Higo, T. Minami, K. Norisuye and S. Umetani, *Anal. Chem.*, 2008, 6267–6273.
46 D. Yeghicheyan, J. Carignan, M. Valladon, M. B. Le Coz, F. Le Cornec, M. Castrec-Rouelle, M. Robert, L. Aquilina, E. Aubry, C. Churlaud, A. Dia, S. Deberdt, B. Dupr, R. Freydier, G. Gruau, O. Henin, A. M. de Kersabiec, J. Mace, L. Marin, N. Morin, P. Petitjean and E. Serrat, *Geostand. Newsl.*, 2001, **25**, 465–474.
47 A. Heimburger, M. Tharaud, F. Monna, R. Losno, K. Desboeufs and E. B. Nguyen, *Geostand. Geoanal. Res.*, 2012, DOI: 10.1111/j.1751-908X.2012.00185.x.
48 S. Kulaksız and M. Bau, *Environ. Int.*, 2011, **37**, 973–979.
49 S. N. Willie and R. E. Sturgeon, *Spectrochim. Acta, Part B*, 2001, **56**, 1707–1716.
50 N. Freslon, G. Bayon, D. Birot, C. Bollinger and J. A. Barrat, *Talanta*, 2011, **85**, 582–587.
51 M. G. Lawrence and B. S. Kamber, *Geostand. Geoanal. Res.*, 2007, **31**, 95–103.
52 K. Pahnke, T. van de Flierdt, K. M. Jones, M. Lambelet, S. R. Hemming and S. L. Goldstein, *Limnol. Oceanogr.: Methods*, 2012, **10**, 252–269.
53 R. Bolhar, B. S. Kamber, S. Moorbath, C. M. Fedo and M. J. Whitehouse, *Earth Planet. Sci. Lett.*, 2004, **222**, 43–60.
54 H. J. W. De Baar, M. P. Bacon, P. G. Brewer and K. W. Bruland, *Geochim. Cosmochim. Acta*, 1985, **49**, 1943–1959.

